Optical Surface Properties and Morphology of MgO and CaO Nanocrystals

Slavica Stankic,[†] Johannes Bernardi,[‡] Oliver Diwald,*[,†] and Erich Knözinger[†]

Institute of Materials Chemistry, Vienna University of Technology, Veterinärplatz 1/GA, A-1210 Vienna, Austria, and University Service Centre for Transmission Electron Microscopy, Vienna University of Technology, Wiedner Hauptstrasse 8-10/137, A-1040 Vienna, Austria

Received: March 21, 2006; In Final Form: May 16, 2006

Optical absorption and photoluminescence emission properties of dehydroxylated MgO and CaO nanocrystals are discussed with respect to particle morphology and size. On MgO nanocubes with pronounced corner and edge features two emission bands at 3.4 and 3.3 eV result from the excitation of 4-coordinated surface O_{4C}^{2-} anions in edges at 5.4 eV and of regular oxygen-terminated corners at 4.6 eV, respectively. Morphologically ill-defined CaO particles are a factor of 5 larger, do not display regular corner features, and show only one photoluminescence emission band at 3.0 eV. The associated excitation spectrum indicates electronic excitations above the energy required to excite regular oxygen-terminated CaO corners. It is concluded that in the case of morphologically well-defined MgO nanocubes variations in the next coordination of oxygen-terminated corners can effectively be probed by photoluminescence spectroscopy and thus allows for discrimination between 3-coordinated surface O^{2-} in regular corner sites and kinks.

Introduction

The interaction between light and highly dispersed oxide materials is fundamentally important in photocatalysis,[1−3] photoelectrochemistry,[4−6] sensor technology,[7,8] and microelectronics and materials processing.[9] Furthermore, surface functionalization of nanocrystalline oxide materials can lead to unexpected optical properties[10] and makes them promising candidates for inorganic phosphors.[11] Finally, a variety of optical spectroscopies have been employed for the characterization of chemically reactive surface sites in the field of heterogeneous catalysis.[12]

As highly dispersed alkaline earth oxides (AEOs) exhibit many different local surface structures, their identification is a complex task. However, due to the ionicity and simple cubic structure, AEOs constitute a unique model system for surface science studies on insulating metal oxides.[13−17] Furthermore, the availability of diverse production techniques has enabled the observation of different morphology-dependent surface characteristics.[18−25] Recently, the morphological properties of AEOs as characterized by transmission electron microscopy (TEM) were connected to the abundance of certain spectroscopic features by various groups. Examples of the successful application of this approach include the study of carbon monoxide[26] and hydrogen[27] adsorption investigated by IR spectroscopy, the characterization of electron traps by electron paramagnetic resonance spectroscopy (EPR),[28] and the assessment of Brönsted basic sites by photoluminescence (PL) spectroscopy.[29]

For MgO and CaO the energies required to generate bulk excitons are 7.7 and 6.8 eV, respectively. However, UV diffuse reflectance spectra of high surface area materials reveal optical absorptions at significantly lower energies.[30−33] The data listed in Table 1 were obtained on two types of samples which were either produced via the thermal decomposition of hydroxides or carbonates ($MeO_{ex-hydroxide}$, $MeO_{ex-carbonate}$)[33] or via the chemical vapor deposition technique (MeO_{CVD}).[10,34]

TABLE 1: Absorption Energies which Were Measured on Dehydroxylated, Highly Dispersed MgO and CaO Powders and Are Attributed to the Electronic Excitation of Surface Oxygen Anions O^{2-} of Different Coordination States[a]

E, eV	$MgO_{ex-hydroxide}$	$CaO_{ex-carbonate}$	MgO_{CVD}	CaO_{CVD}
E_{III} (O_{5C}^{2-})	6.6	5.5	not measured	5.3
E_{II} (O_{4C}^{2-})	5.75	4.4	5.3−5.7[b]	4.4
E_{I} (O_{3C}^{2-})	4.6	3.75	4.6	-

[a] The data for ex-hydroxide/ex-carbonate material and for MeO_{CVD} were taken from refs 33 and 10, respectively. [b] The indicated energy range is due to the fact that the position of the corresponding absorption maximum depends on particle size and shifts with decreasing edge lengths to lower energies.[34]

Garrone et al.[33] related the reduced local Madelung constants at low-coordinated O^{2-} ions to the optical absorption bands listed in Table 1. Derived from a purely electrostatic picture, it was suggested that the energy required to generate an excited surface state, which corresponds to a partial transfer of a surface oxygen electron to its immediate surrounding, decreases with the coordination number of the respective anion.[35] This trend, i.e., dependence of the excitation energy on the number of adjacent cations surrounding the low-coordinated surface anion, has been supported theoretically with excitation energies which were computed for several defects and structural features at the MgO surface.[16,36]

On high surface area AEOs photoluminescence (PL) emission induced by UV light with wavelengths above vacuum UV ($\lambda > 200$ nm, $h\nu < 6.2$ eV) exclusively stems from surface ions.[11,26,29,37−40] The lack of consensus about PL emission data in experimental literature is attributed to the fact that PL emission critically depends on morphology[40] and the residual hydroxylation state of the oxide material[29,41,42] which, in turn, demonstrates that photoluminescence spectroscopy is an especially sensitive technique for the investigation of surface sites.

* Address correspondence to this author. E-mail: odiwald@mail.zserv.tuwien.ac.at. Fax: 011-43-1-25077-3890.

[†] Institute of Materials Chemistry, Vienna University of Technology.

[‡] University Service Centre for Transmission Electron Microscopy, Vienna University of Technology.

10.1021/jp061741a CCC: $33.50
Published on Web 06/28/2006

Emission spectra of dehydroxylated MgO samples contain broad features with maxima in the range between 2.5 and 4.0 eV.[43−45] Whereas some authors have explained excitation and emission events in terms of activation and deactivation steps at the same type of surface site,[29,46] others have suggested that only 3-coordinated oxygen anions act as light emitting sites irrespective of the excitation energy and thus irrespective of the nature of the originally excited center.[45,47] The latter approach requires the presence of mobile surface excitons which enable energy transfer from excited O_{5C}^{2-} or O_{4C}^{2-} sites to O_{3C}^{2-} corners which become active as light emission sites. In fact, theoretical calculations revealed that the localization of an excited state clearly depends on the coordination state and the electronic structure of the respective ion.[36] On the basis of calculated excitation energies for various sites of the crystallite, exciton transfer from the bulk or the (100) surface to less coordinated edge and/or corner sites is expected.

In summary, it should be emphasized that despite more than 25 years of intensive spectroscopic studies of the optical properties of isostructural AEOs, a consistent understanding of the mechanisms of excitation, relaxation, and emission has so far not been reached. The major reasons for this are insufficient coherence between absorption and photoluminescence studies on one hand and a lack of reliable theoretical data on the other. Quantum chemical computations on MgO surface arrays which are likely to render relevant support for the interpretation of the respective absorption and emission spectra were carried out only recently.[36,48,49]

Provided the particles prepared from different isostructural AEOs adopt similar morphology and particle size, the surface electronic properties of MgO, CaO, SrO, and BaO should exhibit an unambiguous trend.[18,26] Unfortunately, the thermal stability of dispersed AEOs decreases in the above given order. As a consequence of thermal activation, which is indispensable for surface purification, the resulting CaO, SrO, and BaO particles are much larger in size and are expected to exhibit altered morphology as compared to MgO particles. It has been found that chemical vapor deposition (CVD) provides unprecedented advantages in producing morphologically well-defined nanoparticles as model systems.[24,50] A previously undetected PL emission band at 3.3 eV was preferentially observed on smaller MgO cubes with edge lengths $d < 10$ nm and is attributed to a radiative deactivation process in oxygen terminated regular corners.[34] Such sites can be characterized as O_{3C}^{2-} ions surrounded by three (001) terraces and are expected to be different from less regular 3-coordinated sites such as kinks.[16]

MgO and CaO are isostructural oxides with lattice constants of 2.1 and 2.4 Å, respectively. In the present investigation, we have carried out an in-depth analysis of photoluminescence properties of these oxides which both were produced by CVD. Detailed band fitting analysis was employed to obtain reliable excitation spectra which were then compared to the corresponding absorption spectra measured by UV diffuse reflectance spectroscopy (Table 1). A microstructural analysis of MgO and CaO nanocrystals by TEM was included in order to discuss the observed light emission in terms of selective excitation of certain topographic surface elements such as corner and edge features.

Experimental Section

MgO and CaO samples were prepared by the chemical vapor deposition technique (CVD) based on the reaction of metal vapor with oxygen within a flow reactor system. Details about this production technique are given elsewhere.[50,51] Spectroscopic measurements were carried out at room temperature with use of quartz glass cells which guarantee high vacuum conditions better than $p < 10^{-6}$ mbar. The sample material was subjected to thermal treatment up to 1173 K and pressures below $<10^{-5}$ mbar. First, the sample was heated at a rate of 5 deg·min^{-1} to 873 K and exposed at this temperature to oxygen to remove organic contaminants. Finally, the sample temperature was raised to 1173 K at pressures $p < 5 \times 10^{-6}$ mbar and kept at this temperature for 1−2 h for total dehydroxylation of the sample surface as judged by IR spectroscopy for both types of oxides.[52,53] Comparable masses of both oxides were used for spectroscopic measurements and the powder densities were of the same order of magnitude as judged from the volume occupied by the powder. An estimate of the number of crystallites which are reached by the excitation beam and thus the number of emission events cannot be given because of light scattering effects between particles which cannot be quantified.

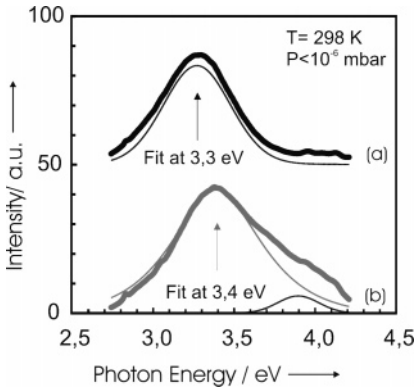

Figure 1. Room-temperature photoluminescence emission spectra of MgO nanocubes after excitation at (a) 4.6 and (b) 5.4 eV.

The presented UV-diffuse reflectance spectra were acquired by using a Perkin-Elmer Lambda 15 spectrophotometer equipped with an integrating sphere and converted to absorption spectra via the Kubelka−Munk transform procedure. A pulsed Xe discharge lamp served as excitation light source in a Perkin-Elmer LS 50B system for photoluminescence measurements. The UV output from the Xe source falls off rapidly at wavelengths below 240 nm and a rhodamine correction curve that is valid in the range between 230 and 630 nm was employed for the correction of the reference multiplier within the spectrometer system. For these reasons, the measured emission intensities at excitation energies above 5.2 eV ($\lambda < 240$ nm) are associated with enhanced systematic errors.

To derive band intensities from the emission features curve fitting was performed with the GRAMS software.[54] For checking the reliability of the fitting procedure, we varied the position of the simulation band maxima, which only reduced the quality of the fit, but did not change the position of the derived excitation maxima. After spectroscopy experiments, small amounts of the metal oxide powders were cast on a holey carbon grid for investigation with a TECNAI F20 analytical transmission electron microscope equipped with a field emission electron source and a S-Twin objective lens. Images were recorded with a Gatan 794 MultiScan camera.

Results

Emission spectra obtained on MgO nanocubes are plotted in Figure 1. Excitation at 5.4 and 4.6 eV produces emission bands with maxima at 3.4 and 3.3 eV, respectively. The positions of the maxima are too closely spaced to measure a well-resolved excitation spectrum directly. Consequently, a systematic band fitting analysis of the emission spectra was carried out. Emission

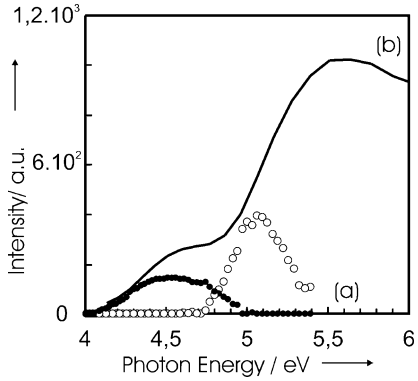

Figure 2. Optical surface properties of MgO nanocubes: (a) photoluminescence excitation spectra of MgO nanocubes associated with the emission bands at 3.3 (full circles) and 3.4 eV (open circles). For comparison, a UV diffuse reflectance spectrum (Kubelka−Munk function) is plotted in part b (for this measurement the sample was exposed to 10 mbar of O_2 to suppress luminescence). The ordinate scalings of parts a and b are arbitrary.

spectra were recorded with use of monochromatic excitation in the range between 4.0 and 5.5 eV.[55] The resulting data were then submitted to a curve fitting routine. Essentially three Gaussian profiles with a full width at half-maximum (fwhm) of 0.7 eV fit the entire set of emission spectra (Figure 1): the features measured after excitation at 4.6 eV (Figure 1a) and 5.4 eV (Figure 1b) were reproduced by Gaussian curves at 3.3 and 3.4 eV, respectively, as well as a smaller contribution at 3.9 eV, which was found to be an experimental artifact.[56]

Intensities for the 3.3 and 3.4 eV bands were determined by integration of the fit bands. In Figure 2a these values are plotted as a function of excitation energy and compared to the diffuse reflectance spectrum in Figure 2b. For the emission at 3.3 eV the corresponding excitation curve has a maximum at 4.6 eV that coincides with the low-energy shoulder of the optical absorption (Figure 2b).[34] The excitation curve is related to the 3.4 eV emission (Figure 2a) peaks at 5.1 eV and is embedded in the low energy part of the much broader absorption feature centered at 5.6 eV (Figure 2b). The excitation band at 4.6 eV is significantly broadened compared to that at 5.1 eV. At the present, this issue remains open and is the subject of an ongoing investigation.

In the case of dehydroxylated CaO particles, emission spectra were recorded with excitation energies between 5.2 and 3.7 eV. In fact, 3.7 eV corresponds to the minimum excitation energy that is associated with significant photoluminescence emission. For the entire excitation energy range, there is only one emission band with a maximum at 3.0 eV detectable, the shape of which is also excitation energy independent (Figure 3). The associated excitation spectrum (Figure 4a) reveals one asymmetric curve, which suggests that more than one excitation process contributes to the photoluminescence emission at 3.0 eV. In fact, the spectrum in Figure 4a can be decomposed into two constituents at 4.2 and 4.7 eV as demonstrated by Figure 4c. It is interesting to note that for ex-carbonate CaO a shoulder at 3.75 eV in the UV diffuse reflectance spectra (Table 1) was reported in ref 33. Such a feature has also been observed in the course of our studies when thermal sample activations between 800 and 1100 K were applied. However, such a treatment is not sufficient for perfect surface dehydroxylation of the CVD material. In the photoluminescence study of ref 45, which was carried out independently from the UV DR investigation of ref 33, a band at 4.46 eV and a shoulder at 4.0 eV were observed as excitation features for an emission band at 3.0 eV. This is in line with our results.

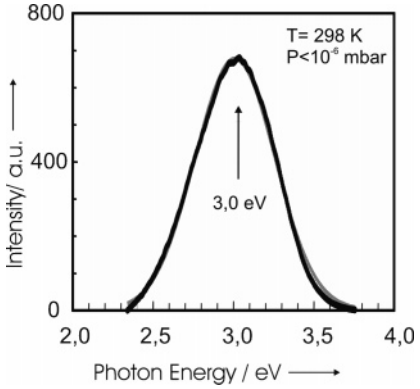

Figure 3. Emission spectrum of dehydroxylated CaO nanoparticles after excitation at 4.3 eV. The experimentally measured spectrum is perfectly reproduced by one Gaussian profile with a maximum at 3.0 eV and a full width at half-maximum of 0.7 eV.

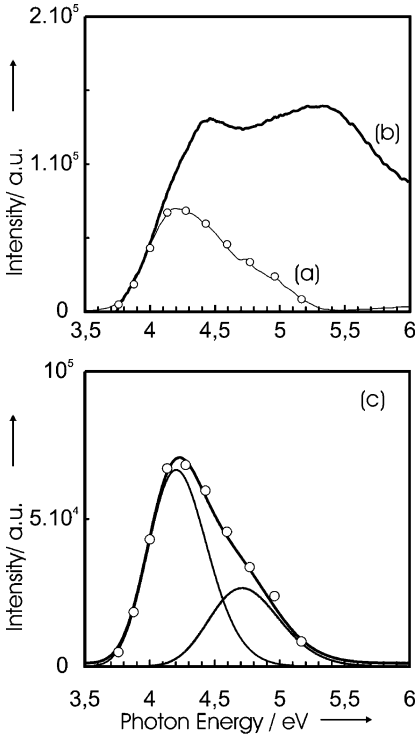

Figure 4. Optical surface properties of CaO particles: the excitation spectrum (a) is obtained in two different ways: by directly measuring the emission intensity at 3.0 eV on tuning the excitation monochromator (solid line) and by plotting the integral emission intensities as a function of the excitation energy (open circles). For comparison, an optical absorption spectrum (Kubelka Munk function) of the same material is plotted in part b. The intensity ratio between its plotted absorbance and the excitation spectrum is arbitrary. Part c demonstrates the decomposition of the photoluminescence excitation spectrum in part a into two components with maxima at 4.2 and 4.7 eV.

In the present study, it was found that the CaO emission band intensity exceeds that observed on the corresponding MgO sample (compare parts a and b of Figure 1) by more than 1 order of magnitude. Since the number of emission centers is likely to be smaller for the larger CaO particles as compared to MgO (ref 10 and see below), this effect is attributed to significant differences in the probability for radiative exciton deactivation.

Both MgO and CaO have the cubic rock-salt structure and are expected to display the same surface topographies such as regular corner sites, kink, ledges, edges, and step edges. However, profound differences between the two types of CVD

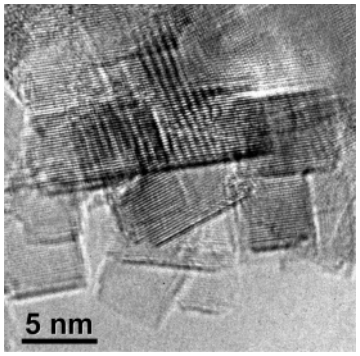

Figure 5. Representative high-resolution TEM image of dehydroxylated MgO nanoparticles obtained after thermal activation ($T = 1173$ K and $p < 10^{-5}$ mbar) of the CVD material.

oxide nanoparticles were observed as a consequence of different thermal stabilities[50] (Figures 5 and 6): first, at 6 nm the average size of the MgO nanoparticles (Figure 5) is significantly smaller than the respective value determined for CaO, which is 27 nm (Figure 6).[10] Second, the morphology of the particles is different. High-resolution TEM images of CVD MgO indicate that the particles are single nanocrystals of essentially cubic shape (Figure 5).[10,26] They preferentially expose low-index (100) faces and terraces and a large proportion of edge and corner sites. CaO particles, on the other hand, are much larger in size and do not adopt cubic shape (Figure 6).[10] Temperature-induced particle coarsening and coalescence has given rise to morphologically ill-defined crystallites which are characterized by the interpenetration of the original cubelets. A close-up of the oxide microstructure is shown in the micrograph on the right-hand side of Figure 6 and points to a complex manifold of surface topographic features. A high concentration of step edges of variable height, ledges, and terraces approximately 5×3 nm^2 in size as well as kink sites can be concluded. Regular corner sites, meaning sites at the intersection between three (100) terraces,[16] seem to be a minority species on the CaO nanocrystals.

Discussion

From a spectroscopic point of view, the major difference between CVD-produced MgO and CaO is given by the number of emission features per oxide. Only for MgO we observe two independent radiative deactivation processes, designated in the following text as Type I and II, with emission band maxima at 3.3 (Type I) and 3.4 eV (Type II). According to Table 1, the Type I process must be related to 3-coordinated corner oxygen anions.[33] In fact, photoinduced processes at oxygen-terminated corners were described theoretically by Shluger et al. via embedded cluster quantum-mechanical calculations.[48,49] For such elements the most intense singlet → singlet transition was found at 4.8 eV. In this most intense transition, electron transfer does not occur from a 3-coordinated O^{2-} corner anion to one of the corner-next Mg^{2+} cations (4C) as adopted in earlier experimental studies.[33] Contrary to expectation it rather involves 4-coordinated O^{2-} anions as electron donor and the 4-coordinated Mg^{2+}cation as the electron-acceptor site. In previous work we have shown that the band at 3.3 eV (Type I) was preferentially observed on cubes with edge lengths smaller than 10 nm. Those also revealed an enhanced absorption band at 4.6 eV as measured by diffuse reflectance spectroscopy.[10] Since the relative abundance of regular corner sites for MgO nanocubes with $d < 10$ nm has to be higher than for those with $d > 10$ nm, this observation supports the assumption that the respective radiative deactivation process occurs in the immediate environment of regular oxygen-terminated corner positions.[34] Different from oxygen-terminated kink sites,[36,39] these sites constitute intersections between three (100) terraces and have 4-coordinated cations as next neighbors.

The photoluminescence process Type II observed on MgO is induced with UV photon energies $h\nu > 4.8$ eV—which, according to the purely electrostatic approach (Table 1), correspond to excitation energies of edge O_{4C}^{2-} anions. The respective excitons are expected to be mobile[36,37,43,45] and, in principle, can transfer to sites with a reduced Madelung potential and thus a coordination smaller than 4. The emission energy of 3.4 eV is in good agreement with other studies carried out on highly dispersed MgO samples which did not exhibit any emission at 3.3 eV (excitation at 4.6 eV).[26,29,43,46]

In the case of the larger and less regular CaO particles, there is neither significant absorption at 3.7 eV (Figure 4a) nor evidence for significant photoluminescence at excitation energies below 3.7 eV (Figure 4b,c). Thus, the absence of a Type I process (Table 1) indicates that the abundance of related oxygen-terminated corner sites and the associated electronic states is too low in order to produce significant photoluminescence emission. The luminescence observed (Figures 3 and 4a) is attributed to the excitation of oxygen ions which are remote from regular oxygen corners, i.e., to oxygen ions in edges or planes (4C or 5C).

On the basis of the differences between MgO and CaO particles in terms of size and surface topography (Figures 5 and 6) we propose a mechanism where essentially three types of surface elements are involved (Scheme 1): (a) oxygen-terminated *regular corner* sites where the next neighbors are 4-coordinated edge Mg^{2+}, (b) *less regular* oxygen-terminated corner sites where the coordination state of the next Mg^{2+} neighbors can exceed four (candidates for such structures can be defective edges where the ideal row of alternating 4C cations and 4C anions is interrupted by point defects such as cation−anion divacancies (Scheme 1), and (c) regular edge sites with 4-coordinated anions.

On both CVD oxides less regular oxygen-terminated corners as well as 4-coordinated anions in edges are present (Figures 5 and 6) and can be efficiently excited. The resulting surface excitons transfer along the edge until they encounter defective sites where radiative deactivation and PL emission can occur (Scheme 1).[16,43−45] Such a mechanism could account for the Type II process (5.1 eV → 3.4 eV) on MgO as well as for the Type II process (4.2/4.7 eV[57] → 3.0 eV) on CaO (Scheme 1). On the other hand, the concentration of regular corner sites is expected to be high only on MgO nanocubes and the respective excitation with 4.6 eV light generates light emission at 3.3 eV. On ill-defined CaO particles the analogous Type I process that should have a maximum at 3.75 eV escapes detection, because of the low abundance of the respective surface sites. The question arises why the direct activation of Type II emission sites (Scheme 1) at photon energies below 5.1 eV (MgO) or below 4.0 eV (CaO) does not give rise to PL emission at room temperature. We speculate that the cross section for such a process is low and nonradiative exciton deactivation predominates at room temperature. Further theoretical work regarding the nature and energies of various excited states as well as low-temperature measurements is needed to elaborate on this hypothesis.

As indicated in the Introduction the emission bands for highly dispersed and dehydroxylated MgO crystals can have quite different energies depending on the method of preparation. This is particularly true for luminescence induced with 4.6 eV light.[29]

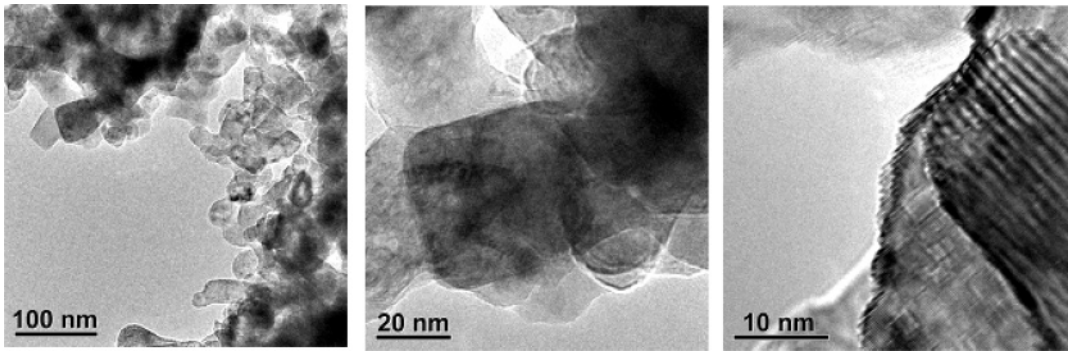

Figure 6. Representative TEM images of dehydroxylated CaO particles obtained after thermal activation ($T = 1173$ K and $p < 10^{-5}$ mbar) of the CVD material.

SCHEME 1: Energies for Photoluminescence Excitation and Emission Processes Observed on MgO Nanocubes ($d = 6$ nm) and on Morphologically Less Regular CaO Nanoparticles ($d = 27$ nm)[a]

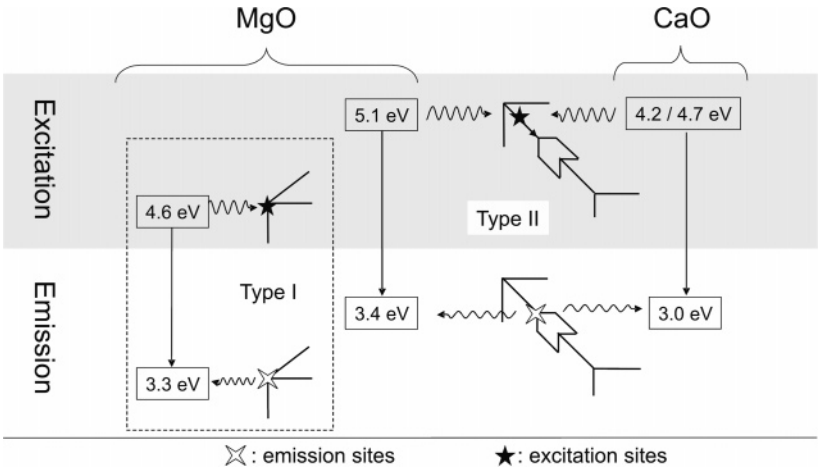

[a] Surface elements which are proposed to be involved in the generation (excitation sites) and deactivation of excitons (emission sites) are schematized.

High surface area MgO obtained from solution-based synthesis techniques and subjected to careful thermal activation procedures is always characterized by much larger primary units composed of interpenetrated cubic substructures. Characteristic TEM images are presented in refs 26−29. These MgO structures are comparable to those observed for CVD CaO (Figure 6) which do not reveal significant PL emission upon excitation of 3C sites with 3.7 eV (Scheme 1). On this basis, the exclusive observation of the 3.3 eV band on MgO nanocubes is attributed to the extraordinary morphology of the CVD material.

We should note that for both MgO and CaO the excitation maxima derived from photoluminescence spectroscopy do not coincide with those of the respective absorption spectra (Figures 2 and 4). Excitations at higher energies are less effective concerning photoluminescence emission. These observations are not understood at the present and, once more, point to the high complexity associated with photoluminescence processes on polycrystal surfaces where various surface elements can contribute to the absorption and emission of light. As pointed out by Cox and Williams,[58] the Madelung potential model does not entirely explain the shift of surface exciton energy with respect to the bulk.[33,35] For alkali halides it could have been shown that experimentally observed surface exciton shifts are in fact much larger than those derived from the difference between Madelung potentials at the surface and in the bulk. More significant contributions arise from quantum effects, such as the topology of the excited electron wave function.[59] Furthermore, as emphasized by recent electronic structure calculations carried out for MgO,[48,49] every surface element is composed of a number of ions rather than one low coordinated O^{2-} anion alone and consequently has various excited states, connected to electronic transitions of distinct energies and transition probabilities.

Our understanding of electronic surface structure on polycrystals needs to be expanded, e.g., via a more systematic look over the family of alkaline earth oxides. Recent advances in morphology control over unsupported nanostructures allow for the deliberate enhancement or depletion of microstructural characteristics. This opens up new opportunities for the endeavor to connect topographic surface features on oxides to their spectroscopic properties and, therefore, to develop our understanding of photoinduced processes on oxide surfaces.

Conclusions

We have investigated the photoluminescence properties of dehydroxylated MgO and CaO nanocrystals at $p < 10^{-6}$ mbar. Essentially two independent photoluminescence processes, Type I and II, can be observed on MgO nanoparticles which adopt cubic shape and display an enhanced abundance of both surface edges and regular cube corner sites, as suggested by the corresponding TEM images. With excitation at $h\nu_{exc} = 4.6$ eV and light emission at $h\nu_{em} = 3.3$ eV the Type I process is attributed to the direct electronic activation and deactivation of regular oxygen-terminated corner sites. The second process, Type II, with excitation at $h\nu_{exc} = 5.1$ eV and emission at $h\nu_{em} = 3.4$ eV, has a larger Stokes shift and is ascribed to the activation of 4-coordinated anions in edges followed by energy transfer along step edges and exciton deactivation at less regular oxygen-terminated corner sites.

On the isostructural but larger CaO particles with ill-defined particle morphology, photoluminescence processes with $h\nu_{exc} = 4.7$ and 4.2 eV $\rightarrow h\nu_{em} = 3.0$ eV which are analogous to Type II on MgO are measured. The absence of the Type I process that corresponds to the direct excitation and deactivation of regular corner sites is explained by their low abundance on CaO nanocrystals. Furthermore, it was found that photoluminescence effects on CaO are more than a factor of 10 higher in intensity compared to MgO even though the abundance of surface sites is, due to the larger size of the particles, likely to be significantly smaller in CaO samples of the same molar amount.

Acknowledgment. This work was financially supported by Fonds zur Förderung der Wissenschaftlichen Forschung (FWF) P 17770-N11 and the Hochschuljubiläumsstiftung der Stadt Wien (H-175/2001) both of which are gratefully acknowledged. We also thank P. V. Sushko for very useful discussions and his critical comments on the manuscript, as well as Lindsay R. Merte for comments and proofreading.

References and Notes

(1) Linsebigler, A. L.; Lu, G. Q.; Yates, J. T., Jr. *Chem. Rev.* **1995**, *95*, 735.
(2) Hoffmann, M. R.; Martin, S. T.; Choi, W. Y.; Bahnemann, D. W. *Chem. Rev.* **1995**, *95*, 69.
(3) Rajh, T.; Makarova, O. V.; Thurnauer, M. C.; Cropek, D. In *Synthesis, Functionalization and Surface Treatment of Nanoparticles*; Baraton, M. I., Ed.; American Science Publishers: Stevenson Ranch, CA, 2003.
(4) O'Regan, B.; Grätzel, M. *Nature* **1991**, *353*, 737.
(5) Bisquert, J.; Cahen, D.; Hodes, G.; Ruhle, S.; Zaban, A. *J. Phys. Chem. B* **2004**, *108*, 8106.
(6) Watson, D. F.; Meyer, G. J. *Annu. Rev. Phys. Chem.* **2005**, 56, 119.
(7) Mor, G. K.; Carvalho, M. A.; Varghese, O. K.; Pishko, M. V.; Grimes, C. A. *J. Mater. Res.* **2004**, 19, 628.
(8) Shukla, S.; Agrawal, R.; Cho, H. J.; Seal, S.; Ludwig, L.; Parish, C. *J. Appl. Phys.* **2005**, 97, 054307.
(9) Bäuerle, D. *Laser Processing and Chemistry*; Springer-Verlag: Berlin, Germany, 2000.
(10) Stankic, S.; Sterrer, M.; Bernardi, J.; Diwald, O.; Knözinger, E. *Nano Lett.* **2005**, *5*, 1889.
(11) Abrams, B. L.; Holloway, P. H. *Chem. Rev.* **2005**, *104*, 5783.
(12) Anpo, M.; Che, M. *Adv. Catal.* **1999**, *44*, 119.
(13) Henrich, V. E.; Cox, P. A. *The Surface Science of Metal Oxides*; Cambridge University Press: Cambridge, UK, 1996.
(14) Sterrer, M.; Fischbach, E.; Risse, T.; Freund, H. J. *Phys. Rev. Lett.* **2005**, *94*, 186101.
(15) Barth, C.; Henry, C. R. *Phys. Rev. Lett.* **2003**, *91*, 196102.
(16) Sushko, P. V.; Gavartin, J.; Shluger, A. L. *J. Phys. Chem. B* **2002**, *106*, 2269.
(17) Sterrer, M.; Berger, T.; Diwald, O.; Knözinger, E.; Sushko, P. V.; Shluger, A. L. *J. Chem. Phys.* **2005**, *123*, 064714.
(18) Zecchina, A.; Lofthouse, M. G.; Stone, F. S. *J. Chem. Soc., Faraday Trans. 1* **1975**, *71*, 1476.
(19) Zecchina, A.; Scarano, D. *Stud. Surf. Sci. Catal.* **1985**, *21*, 71.
(20) Klabunde, K. J.; Stark, J.; Koper, O.; Mochs, C.; Park, D. G.; Decker, S.; Jiang, Y.; Lagadic, I.; Zhang, D. J. *J. Phys. Chem.* **1996**, *100*, 2142.
(21) Koper, O. B.; Lagadic, I.; Volodin, A.; Klabunde, K. J. *Chem. Mater.* **1997**, *9*, 2468.
(22) Dohnalek, Z.; Smith, R. S.; Kay, B. D. *J. Phys. Chem. B* **2002**, *106*, 8360.
(23) Dohnalek, Z.; Kimmel, G. A.; McCready, D. E.; Young, J. S.; Dohnalkova, A.; Smith, R. S.; Kay, B. D. *J. Phys. Chem. B* **2002**, *106*, 3526.
(24) Knözinger, E.; Diwald, O.; Sterrer, M. *J. Mol. Catal. A Chem.* **2000**, *162*, 83.
(25) Sterrer, M.; Berger, T.; Stankic, S.; Diwald, O.; Knözinger, E. *Chem. Phys. Chem.* **2004**, *5*, 1695.
(26) Spoto, G.; Gribov, E. N.; Ricchiardi, G.; Damin, A.; Scarano, D.; Bordiga, S.; Lamberti, C.; Zecchina, A. *Prog. Surf. Sci.* **2004**, *76*, 71.
(27) Gribov, E. N.; Bertarione, S.; Scarano, D.; Lamberti, C.; Spoto, G.; Zecchina, A. *J. Phys. Chem. B* **2004**, *108*, 16174.
(28) Chiesa, M.; Paganini, M. C.; Spoto, G.; Giamello, E.; Di Valentin, C.; Del Vitto, A.; Pacchioni, G. *J. Phys. Chem. B* **2005**, *109*, 7314.
(29) Bailly, L.-M.; Costentin, G.; Lauron-Pernot, H.; Krafft, J. M.; Che, M. *J. Phys. Chem. B* **2005**, *109*, 2404.
(30) Zecchina, A.; Stone, F. S. *J. Chem. Soc., Faraday Trans. 1* **1976**, *72*, 2364.
(31) Zecchina, A.; Lofthouse, M. G.; Stone, F. S. *J. Chem. Soc., Faraday Trans. 1* **1975**, *71*, 1476.
(32) Nelson, R. L.; Hale, J. W. *Discuss. Faraday Soc.* **1971**, *52*, 77.
(33) Garrone, E.; Zecchina, A.; Stone, F. S. *Philos. Mag.* **1980**, *42* B, 683.
(34) Stankic, S.; Müller, M.; Sterrer, M.; Bernardi, J.; Diwald, O.; Knözinger, E. *Angew. Chem., Int. Ed.* **2005**, *44*, 4917.
(35) Levine, J. D.; Mark, P. *Phys. Rev.* **1966**, *144*, 751.
(36) Shluger, L.; Sushko, P. V.; Kantorovic, L. N. *Phys. Rev. B* **1999**, *59*, 2417.
(37) Coluccia, S.; Tench, A. J. *J. Chem. Soc., Faraday Trans. 1* **1983**, *79*, 1881.
(38) Sterrer, M.; Diwald, O.; Berger, T.; Knözinger, E. *J. Am. Chem. Soc.* **2003**, *125*, 195.
(39) Sushko, P. V.; Shluger, A. L.; Catlow, C. R. A. *Surf. Sci.* **2000**, *450*, 153.
(40) MacLean, S. G.; Duley, W. W. *J. Phys. Chem. Solids* **1984**, *45*, 227.
(41) Anpo, M.; Yamada, Y.; Kubokawa, Y.; Coluccia, S.; Zecchina, A.; Che, M. *J. Chem. Soc., Faraday Trans. 1* **1988**, *84*, 751.
(42) Hacquart, R.; Krafft, J.-M.; Costentin, G.; Jupille, J. *Surf. Sci.* **2005**, *595*, 172.
(43) Coluccia, S. In *Adsorption and Catalysis on Oxide Surfaces*; Che, M., Bond, G. C., Eds.: Elsevier: Amsterdam, The Netherlands, 1984; p 9.
(44) Coluccia, S.; Tench, A. J. *Proc. Int. Congr. Catal., 7th* **1980**, 1154.
(45) Coluccia, S.; Deane, A. M.; Tench, A. J. *J. Chem. Soc., Faraday Trans. 1* **1978**, *74*, 2913.
(46) Bailly, M. L.; Costentin, G.; Krafft, J. M.; Che, M. *Catal. Lett.* **2004**, *92*, 101.
(47) Coluccia, S.; Tench, A. J. *J. Chem. Soc., Faraday Trans. 1* **1983**, *79*, 1881.
(48) Trevisanutto, P. E.; Sushko, P. V.; Shluger, A. L.; Beck, K. M.; Henyk, M.; Joly, A. G.; Hess, W. P. *Surf. Sci.* **2005**, *593*, 210.
(49) Hess, W. P.; Joly, A. L.; Beck, K. M.; Henyk, M.; Sushko, P. V.; Trevisanutto, P. E.; Shluger, A. L. *J. Phys. Chem. B* **2005**, *109*, 19563.
(50) Hofmann, P.; Knözinger, E.; Diwald, O.; Mustafa, A. *Ber. Bunsen-Ges. Phys. Chem.* **1997**, *101*, 1722.
(51) Becker, A.; Benfer, S.; Hofmann, P.; Jacob, K.-H.; Knözinger, E. *Ber. Bunsen-Ges. Phys. Chem.* **1995**, *99*, 1328.
(52) Hofmann, P. Ph.D. Thesis, Vienna University of Technology, Vienna, 1997.
(53) Diwald, O.; Sterrer, M.; Knözinger, E. *PhysChemChemPhys* **2002**, *4*, 2811.
(54) *GRAMS/32®Spectral Notebase*, Version 4.01; Galactic Industries Corporation, 1991−1996.
(55) There is no significant photoluminescence emission excitation at energies below 4.0 eV.
(56) Different from the two emission bands centered at 3.3 and 3.4 eV and from the study of Hacquart et al.,[42] who observed an emission band at the same energy—the intensity of this feature is not affected by O_2 and other gases. Use of interference filters, which suppress disturbing stray light effects, leads to the total loss of this feature and reveals its artificial nature.
(57) Either the presence of more than one characteristic 4C site/5C site or a second electronic transition associated with the same surface element can account for this double excitation spectrum.
(58) Cox, P. A.; Williams, A. A. *Surf. Sci.* **1986**, *175*, L782
(59) Hess, W. P.; Joly, A. G.; Beck, K. M.; Sushko, P. V.; Shluger, A. L. *Surf. Sci.* **2004**, *564*, 62.